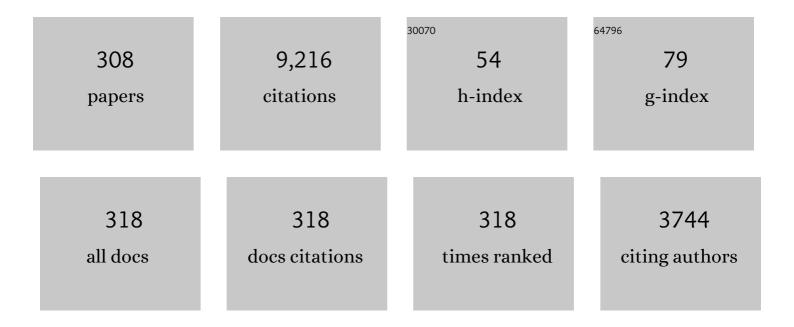
## Pascal Laugier

List of Publications by Year in descending order

Source: https://exaly.com/author-pdf/5983438/publications.pdf Version: 2024-02-01



#	Article	IF	CITATIONS
1	Inverse Problem in Resonant Ultrasound Spectroscopy With Sampling and Optimization: A Comparative Study on Human Cortical Bone. IEEE Transactions on Ultrasonics, Ferroelectrics, and Frequency Control, 2022, 69, 650-661.	3.0	0
2	Clinical Devices for Bone Assessment. Advances in Experimental Medicine and Biology, 2022, 1364, 35-53.	1.6	2
3	Axial Transmission: Techniques, Devices and Clinical Results. Advances in Experimental Medicine and Biology, 2022, 1364, 55-94.	1.6	0
4	Bulk Wave Velocities in Cortical Bone Reflect Porosity and Compression Strength. Ultrasound in Medicine and Biology, 2021, 47, 799-808.	1.5	13
5	Cortical bone viscoelastic damping assessed with resonant ultrasound spectroscopy reflects porosity and mineral content. Journal of the Mechanical Behavior of Biomedical Materials, 2021, 117, 104388.	3.1	6
6	Application of differential evolution on elasticity measurement of low quality factor materials using FEM-based resonant ultrasound spectroscopy. Journal of the Mechanical Behavior of Biomedical Materials, 2021, 124, 104848.	3.1	3
7	Anisotropic elastic properties of human cortical bone tissue inferred from inverse homogenization and resonant ultrasound spectroscopy. Materialia, 2020, 11, 100730.	2.7	10
8	Particle Swarm Optimization-based Identification of the Elastic Properties in Resonant Ultrasound Spectroscopy. IEEE Transactions on Ultrasonics, Ferroelectrics, and Frequency Control, 2020, 67, 1-1.	3.0	8
9	A resonant frequency retrieving method for low Q-factor materials based on resonant ultrasound spectroscopy. Ultrasonics, 2019, 99, 105971.	3.9	11
10	Computed tomography porosity and spherical indentation for determining cortical bone millimetre-scale mechanical properties. Scientific Reports, 2019, 9, 7416.	3.3	22
11	Elastic constants identification of irregular hard biological tissue materials using FEM-based resonant ultrasound spectroscopy. Journal of the Mechanical Behavior of Biomedical Materials, 2019, 96, 20-26.	3.1	5
12	Homogenization of cortical bone reveals that the organization and shape of pores marginally affect elasticity. Journal of the Royal Society Interface, 2019, 16, 20180911.	3.4	20
13	Anisotropic elastic properties of human femoral cortical bone and relationships with composition and microstructure in elderly. Acta Biomaterialia, 2019, 90, 254-266.	8.3	31
14	Ex vivo cortical porosity and thickness predictions at the tibia using full-spectrum ultrasonic guided-wave analysis. Archives of Osteoporosis, 2019, 14, 21.	2.4	24
15	FEM-based Resonant Ultrasound Spectroscopy Method for Measurement of the Elastic Properties of Irregular Solid Specimens. , 2019, , .		Ο
16	Identification of Stiffness Coefficients in Resonant Ultrasound Spectroscopy Using Particle Swarm Optimization. , 2019, , .		0
17	Elastic properties measurement of human enamel based on resonant ultrasound spectroscopy. Journal of the Mechanical Behavior of Biomedical Materials, 2019, 89, 48-53.	3.1	12
18	<i>In vivo</i> ultrasound imaging of the bone cortex. Physics in Medicine and Biology, 2018, 63, 125010.	3.0	68

#	Article	IF	CITATIONS
19	Dispersive Radon transform. Journal of the Acoustical Society of America, 2018, 143, 2729-2743.	1.1	31
20	Predicting bone strength with ultrasonic guided waves. Scientific Reports, 2017, 7, 43628.	3.3	55
21	Cortical bone elasticity measured by resonant ultrasound spectroscopy is not altered by defatting and synchrotron X-ray imaging. Journal of the Mechanical Behavior of Biomedical Materials, 2017, 72, 241-245.	3.1	12
22	Dispersion characteristics of the flexural wave assessed using low frequency (50–150 kHz) point-contact transducers: A feasibility study on bone-mimicking phantoms. Ultrasonics, 2017, 81, 1-9.	3.9	13
23	A critical assessment of the in-vitro measurement of cortical bone stiffness with ultrasound. Ultrasonics, 2017, 80, 119-126.	3.9	23
24	Quantification of stiffness measurement errors in resonant ultrasound spectroscopy of human cortical bone. Journal of the Acoustical Society of America, 2017, 142, 2755-2765.	1.1	17
25	Assessment of trabecular bone tissue elasticity with resonant ultrasound spectroscopy. Journal of the Mechanical Behavior of Biomedical Materials, 2017, 74, 106-110.	3.1	13
26	Notice of Removal: Bone matrix elastic properties determined by FFT-based inverse homogenization. , 2017, , .		0
27	Notice of Removal: The elastic properties of human cortical bone measured by resonant ultrasound spectroscopy at multiple skeletal sites. , 2017, , .		1
28	Notice of Removal: Relationships between cortical bone quality biomarkers: Stiffness, toughness, microstructure, mineralization, cross-links and collagen. , 2017, , .		1
29	<italic>In Vivo</italic> Characterization of Cortical Bone Using Guided Waves Measured by Axial Transmission. IEEE Transactions on Ultrasonics, Ferroelectrics, and Frequency Control, 2016, 63, 1361-1371.	3.0	51
30	Measurement of dispersion curves of circumferential guided waves radiating from curved shells: Theory and numerical validation. Journal of the Acoustical Society of America, 2016, 139, 790-799.	1.1	4
31	Multichannel wideband mode-selective excitation of ultrasonic guided waves in long cortical bone. , 2016, , .		5
32	Multichannel processing for dispersion curves extraction of ultrasonic axial-transmission signals: Comparisons and case studies. Journal of the Acoustical Society of America, 2016, 140, 1758-1770.	1.1	29
33	Sparse SVD Method for High-Resolution Extraction of the Dispersion Curves of Ultrasonic Guided Waves. IEEE Transactions on Ultrasonics, Ferroelectrics, and Frequency Control, 2016, 63, 1514-1524.	3.0	61
34	Genetic algorithms-based inversion of multimode guided waves for cortical bone characterization. Physics in Medicine and Biology, 2016, 61, 6953-6974.	3.0	42
35	A method for the measurement of dispersion curves of circumferential guided waves radiating from curved shells: experimental validation and application to a femoral neck mimicking phantom. Physics in Medicine and Biology, 2016, 61, 4746-4762.	3.0	6
36	Elasticity–density and viscoelasticity–density relationships at the tibia mid-diaphysis assessed from resonant ultrasound spectroscopy measurements. Biomechanics and Modeling in Mechanobiology, 2016, 15, 97-109.	2.8	45

#	Article	IF	CITATIONS
37	A free plate model can predict guided modes propagating in tubular bone-mimicking phantoms. Journal of the Acoustical Society of America, 2015, 137, EL98-EL104.	1.1	25
38	Quantification of nonlinear elasticity for the evaluation of submillimeter crack length in cortical bone. Journal of the Mechanical Behavior of Biomedical Materials, 2015, 48, 210-219.	3.1	8
39	Bayesian normal modes identification and estimation of elastic coefficients in resonant ultrasound spectroscopy. Inverse Problems, 2015, 31, 065010.	2.0	43
40	Distribution of mesoscale elastic properties and mass density in the human femoral shaft. Connective Tissue Research, 2015, 56, 120-132.	2.3	11
41	Prospective discrimination of vertebral fractures by axial transmission ultrasound using optimized first arriving signal velocity measurements. , 2015, , .		2
42	An anisotropic bilayer model to gain insight into in-vivo guided wave measurements. , 2015, , .		0
43	A genetic algorithms-based optimization method for estimating thickness and porosity of cortical bone from guided wave measurements. , 2015, , .		0
44	Sparse inversion SVD method for dispersion extraction of ultrasonic guided waves in cortical bone. , 2015, , .		1
45	An introduction to measurements of human cortical bone elasticity using Resonant Ultrasound Spectroscopy. , 2015, , .		0
46	Numerical estimation of femoral neck cortical bone thickness based on time domain topological energy and sparse signal approximation. , 2015, , .		0
47	Discrimination of fractured from non-fractured post-menopausal women using guided wave-based ultrasound: A pilot clinical study. , 2015, , .		0
48	A Novel Ultrasound Methodology for Estimating Spine Mineral Density. Ultrasound in Medicine and Biology, 2015, 41, 281-300.	1.5	79
49	To what extent can cortical bone millimeter-scale elasticity be predicted by a two-phase composite model with variable porosity?. Acta Biomaterialia, 2015, 12, 207-215.	8.3	20
50	Non Destructive Characterization of Cortical Bone Micro-Damage by Nonlinear Resonant Ultrasound Spectroscopy. PLoS ONE, 2014, 9, e83599.	2.5	31
51	Resonant ultrasound spectroscopy for viscoelastic characterization of anisotropic attenuative solid materials. Journal of the Acoustical Society of America, 2014, 135, 2601-2613.	1.1	51
52	Measuring the wavenumber of guided modes in waveguides with linearly varying thickness. Journal of the Acoustical Society of America, 2014, 135, 2614-2624.	1.1	29
53	Accurate measurement of guided modes in a plate using a bidirectional approach. Journal of the Acoustical Society of America, 2014, 135, EL15-EL21.	1.1	19
54	Ultrasound tissue characterizationby generalized GAMMA MRF model. , 2014, , .		0

#	Article	IF	CITATIONS
55	In vivo measurements of guided waves at the forearm. , 2014, , .		3
56	Detection of elastic guided waves using an axial transmission method: Performance comparison between PZT and cMUT technologies. , 2014, , .		1
57	Circumferential guided wave measurements of a cylindrical fluid-filled bone-mimicking phantom. Journal of the Acoustical Society of America, 2014, 135, 994-1001.	1.1	5
58	Preface. Ultrasonics, 2014, 54, 1123-1124.	3.9	2
59	Non-destructive assessment of human ribs mechanical properties using quantitative ultrasound. Journal of Biomechanics, 2014, 47, 1548-1553.	2.1	6
60	A hybrid FDTD-Rayleigh integral computational method for the simulation of the ultrasound measurement of proximal femur. Ultrasonics, 2014, 54, 1197-1202.	3.9	3
61	Combined estimation of thickness and velocities using ultrasound guided waves: a pioneering study on in vitro cortical bone samples. IEEE Transactions on Ultrasonics, Ferroelectrics, and Frequency Control, 2014, 61, 1478-1488.	3.0	83
62	A capacitive micromachined ultrasonic transducer probe for assessment of cortical bone. IEEE Transactions on Ultrasonics, Ferroelectrics, and Frequency Control, 2014, 61, 710-723.	3.0	28
63	Wideband dispersion reversal of lamb waves. IEEE Transactions on Ultrasonics, Ferroelectrics, and Frequency Control, 2014, 61, 997-1005.	3.0	36
64	Ultrasound to Assess Bone Quality. Current Osteoporosis Reports, 2014, 12, 154-162.	3.6	68
65	Modeling of Femoral Neck Cortical Bone for the Numerical Simulation of Ultrasound Propagation. Ultrasound in Medicine and Biology, 2014, 40, 1015-1026.	1.5	19
66	Influence of porosity, pore size, and cortical thickness on the propagation of ultrasonic waves guided through the femoral neck cortex: a simulation study. IEEE Transactions on Ultrasonics, Ferroelectrics, and Frequency Control, 2014, 61, 302-313.	3.0	24
67	Anisotropy of dynamic acoustoelasticity in limestone, influence of conditioning, and comparison with nonlinear resonance spectroscopy. Journal of the Acoustical Society of America, 2013, 133, 3706-3718.	1.1	51
68	Coupling of finite difference elastodynamic and semi-analytic Rayleigh integral codes for the modelling of ultrasound propagation at the hip. Proceedings of Meetings on Acoustics, 2013, , .	0.3	0
69	Quantitative ultrasound of cortical bone in the femoral neck predicts femur strength: Results of a pilot study. Journal of Bone and Mineral Research, 2013, 28, 302-312.	2.8	36
70	Three-dimensional quantitative ultrasound for detecting lymph node metastases. Journal of Surgical Research, 2013, 183, 258-269.	1.6	34
71	Accurate measurement of cortical bone elasticity tensor with resonant ultrasound spectroscopy. Journal of the Mechanical Behavior of Biomedical Materials, 2013, 18, 12-19.	3.1	91
72	Probing heterogeneity of cortical bone with ultrasound axial transmission. IEEE Transactions on Ultrasonics, Ferroelectrics, and Frequency Control, 2013, 60, 187-193.	3.0	9

#	Article	IF	CITATIONS
73	Spatial-resolution optimization of 3D high-frequency quantitative ultrasound methods to detect metastatic regions in human lymph nodes. , 2013, , .		1
74	High-frequency quantitative ultrasound approaches for cancer detection in freshly-excised lymph nodes. Proceedings of Meetings on Acoustics, 2013, , .	0.3	0
75	Developement and validation of resonant ultrasound spectroscopy for the measurement of cortical bone elasticity on small cylindrical samples. Proceedings of Meetings on Acoustics, 2013, , .	0.3	1
76	Microfibril Orientation Dominates the Microelastic Properties of Human Bone Tissue at the Lamellar Length Scale. PLoS ONE, 2013, 8, e58043.	2.5	56
77	Nonlinear ultrasound: Potential of the cross-correlation method for osseointegration monitoring. Journal of the Acoustical Society of America, 2012, 132, EL202-EL207.	1.1	5
78	Time reversed elastic nonlinearity diagnostic applied to mock osseointegration monitoring applying two experimental models. Journal of the Acoustical Society of America, 2012, 131, 1922-1927.	1.1	12
79	Comparative investigation of elastic properties in a trabecula using micro-Brillouin scattering and scanning acoustic microscopy. Journal of the Acoustical Society of America, 2012, 132, EL54-EL60.	1.1	16
80	The effect of bone fracture unevenness on ultrasound axial transmission measurements: A pilot 2D simulation study. , 2012, , .		0
81	Measuring viscoelastic properties of cortical bone with resonant ultrasound spectroscopy. , 2012, , .		1
82	Lymph Explorer: A new GUI using 3D high-frequency quantitative ultrasound methods to guide pathologists towards metastatic regions in human lymph nodes. , 2012, , .		2
83	A quantitative ultrasound-based method and device for reliably guiding pathologists to metastatic regions of dissected lymph nodes. , 2012, , .		5
84	Measurement of guided mode wavenumbers in soft tissue–bone mimicking phantoms using ultrasonic axial transmission. Physics in Medicine and Biology, 2012, 57, 3025-3037.	3.0	32
85	Characterization of circumferential guided waves in a cylindrical cortical bone-mimicking phantom. Journal of the Acoustical Society of America, 2012, 131, EL289-EL294.	1.1	11
86	Cortical bone quality assessment using quantitative ultrasound on long bones. , 2012, 2012, 1121-4.		5
87	Three-dimensional quantitative ultrasound to guide pathologists towards metastatic foci in lymph nodes. , 2012, 2012, 1114-7.		2
88	First Application of Axial Speed of Sound to Follow Up Injured Equine Tendons. Ultrasound in Medicine and Biology, 2012, 38, 162-167.	1.5	12
89	Dispersion curve measurements of a fluid filled femoral neck mimicking phantom. , 2012, , .		Ο
90	Axial speed of sound for the monitoring of injured equine tendons: A preliminary study. Journal of Biomechanics, 2012, 45, 53-58.	2.1	8

#	Article	lF	CITATIONS
91	Axial speed of sound is related to tendon's nonlinear elasticity. Journal of Biomechanics, 2012, 45, 263-268.	2.1	25
92	Spatial distribution of tissue level properties in a human femoral cortical bone. Journal of Biomechanics, 2012, 45, 2264-2270.	2.1	42
93	Relative contributions of porosity and mineralized matrix properties to the bulk axial ultrasonic wave velocity in human cortical bone. Ultrasonics, 2012, 52, 467-471.	3.9	23
94	Circumferential guided wave measurement in a cortical bone-mimicking cylindrical phantom. , 2011, , .		0
95	Three-dimensional quantitative high-frequency characterization of freshly-excised human lymph nodes. , 2011, , .		3
96	Impact of attenuation on guided mode wavenumber measurement in axial transmission on bone mimicking plates. Journal of the Acoustical Society of America, 2011, 130, 3574-3582.	1.1	57
97	Poromechanical Models. , 2011, , 83-121.		0
98	Experimental and simulation results on the effect of cortical bone mineralization in ultrasound axial transmission measurements: A model for fracture healing ultrasound monitoring. Bone, 2011, 48, 1202-1209.	2.9	32
99	Change in porosity is the major determinant of the variation of cortical bone elasticity at the millimeter scale in aged women. Bone, 2011, 49, 1020-1026.	2.9	116
100	InÂVivo Gene Transfer into the Ocular Ciliary Muscle Mediated byÂUltrasound and Microbubbles. Ultrasound in Medicine and Biology, 2011, 37, 1814-1827.	1.5	22
101	Measurement of guided mode wave vectors by analysis of the transfer matrix obtained with multi-emitters and multi-receivers in contact. Journal of Physics: Conference Series, 2011, 269, 012003.	0.4	5
102	A determination of the minimum sizes of representative volume elements for the prediction of cortical bone elastic properties. Biomechanics and Modeling in Mechanobiology, 2011, 10, 925-937.	2.8	57
103	An alternative quantitative acoustical and electrical method for detection of cell adhesion process in realâ€time. Biotechnology and Bioengineering, 2011, 108, 947-962.	3.3	17
104	True stress and Poisson's ratio of tendons during loading. Journal of Biomechanics, 2011, 44, 719-724.	2.1	52
105	A two-parameter model of the effective elastic tensor for cortical bone. Journal of Biomechanics, 2011, 44, 1621-1625.	2.1	42
106	Three-Dimensional High-Frequency Backscatter and Envelope Quantification of Cancerous Human Lymph Nodes. Ultrasound in Medicine and Biology, 2011, 37, 345-357.	1.5	139
107	Assessment of anisotropic elasticity of small bone samples with resonant ultrasound spectroscopy: Attenuation does not prevent the measurements. , 2011, , .		8
108	Nonlinear ultrasound monitoring of fatigue microdamage accumulation in cortical bone. , 2011, , .		1

#	Article	IF	CITATIONS
109	Guided mode measurement on bone phantoms with realistic geometry. , 2011, , .		0
110	High-accuracy acoustic detection of nonclassical component of material nonlinearity. Journal of the Acoustical Society of America, 2011, 130, 2654-2661.	1.1	62
111	Non-invasive assessment of human ribs mechanical properties. Computer Methods in Biomechanics and Biomedical Engineering, 2011, 14, 195-196.	1.6	4
112	First application of an axial speed of sound measurement technique in the monitoring of tendon healing. Computer Methods in Biomechanics and Biomedical Engineering, 2011, 14, 257-259.	1.6	0
113	Nonlinear elastodynamics in micro-inhomogeneous solids observed by head-wave based dynamic acoustoelastic testing. Journal of the Acoustical Society of America, 2011, 130, 3583-3589.	1.1	58
114	Bone Overview. , 2011, , 1-28.		3
115	Phase Velocity of Cancellous Bone: Negative Dispersion Arising from Fast and Slow Waves, Interference, Diffraction, and Phase Cancellation at Piezoelectric Receiving Elements. , 2011, , 319-330.		5
116	Linear Ultrasonic Properties of Cortical Bone: In Vitro Studies. , 2011, , 331-360.		6
117	Nonlinear Acoustics for Non-invasive Assessment of Bone Micro-damage. , 2011, , 381-408.		1
118	Introduction to the Physics of Ultrasound. , 2011, , 29-45.		40
119	Quantitative Ultrasound Instrumentation for Bone In Vivo Characterization. , 2011, , 47-71.		19
120	Guided Waves in Cortical Bone. , 2011, , 147-179.		13
121	Numerical Methods for Ultrasonic Bone Characterization. , 2011, , 181-228.		13
122	Scattering by Trabecular Bone. , 2011, , 123-145.		9
123	Nonlinear acoustic resonances to probe a threaded interface. Journal of Applied Physics, 2010, 107, .	2.5	19
124	Multiscale structure-functional modeling of lamellar bone. Proceedings of Meetings on Acoustics, 2010, , .	0.3	2
125	Femur ultrasound (FemUS)—first clinical results on hip fracture discrimination and estimation of femoral BMD. Osteoporosis International, 2010, 21, 969-976.	3.1	47
126	Inhibition of angiogenesis in vitro with soluble copolymers monitored with a quartz crystal resonator. Irbm, 2010, 31, 271-279.	5.6	3

#	Article	IF	CITATIONS
127	Real-time Chirp-Coded Imaging With a Programmable Ultrasound Biomicroscope. IEEE Transactions on Biomedical Engineering, 2010, 57, 654-664.	4.2	17
128	Three-Dimensional High-Frequency Characterization of Cancerous Lymph Nodes. Ultrasound in Medicine and Biology, 2010, 36, 361-375.	1.5	84
129	Computational Evaluation of the Compositional Factors in Fracture Healing Affecting Ultrasound Axial Transmission Measurements. Ultrasound in Medicine and Biology, 2010, 36, 1314-1326.	1.5	32
130	Potential of First Arriving Signal to Assess Cortical Bone Geometry at the Hip with QUS: A Model Based Study. Ultrasound in Medicine and Biology, 2010, 36, 656-666.	1.5	29
131	Adaptive Remodeling of Trabecular Bone Core Cultured in 3-D Bioreactor Providing Cyclic Loading: An Acoustic Microscopy Study. Ultrasound in Medicine and Biology, 2010, 36, 999-1007.	1.5	10
132	Assembling 3D histology volumes from sections of cancerous lymph nodes to match 3D high-frequency quantitative ultrasound images. , 2010, , .		4
133	Measurement of guided mode wave numbers in anisotropic absorbing material: Application to cortical bone evaluation. , 2010, , .		0
134	Experimental investigation of local elastic properties in a trabecula of bovine femur. , 2010, , .		0
135	A Linear Laser Scanner to Measure Cross-Sectional Shape and Area of Biological Specimens During Mechanical Testing. Journal of Biomechanical Engineering, 2010, 132, 105001.	1.3	16
136	Guided wave phase velocity measurement using multi-emitter and multi-receiver arrays in the axial transmission configuration. Journal of the Acoustical Society of America, 2010, 127, 2913-2919.	1,1	92
137	Trabecular and cortical bone separately assessed at radius with a new ultrasound device, in a young adult population with various physical activities. Bone, 2010, 46, 1620-1625.	2.9	38
138	Ultrasonic assessment of the determinants of human cortical bone elasticity: Relative contributions of Haversian porosity and mineralized matrix stiffness. , 2010, , .		0
139	Inverse problems in cancellous bone: Estimation of the ultrasonic properties of fast and slow waves using Bayesian probability theory. Journal of the Acoustical Society of America, 2010, 128, 2940-2948.	1.1	36
140	Measurement of cross-sectional area variations of five equine superficial digital flexor tendons during tension. Computer Methods in Biomechanics and Biomedical Engineering, 2010, 13, 143-144.	1.6	2
141	Simultaneous determination of acoustic velocity and density of a cortical bone slab: ultrasonic model-based approach - correspondence. IEEE Transactions on Ultrasonics, Ferroelectrics, and Frequency Control, 2010, 57, 496-500.	3.0	9
142	Three-dimensional high-frequency spectral and envelope quantification of excised human lymph nodes. , 2010, , .		2
143	Cortical Bone Microelasticity Assessed with Scanning Acoustic Microscopy: Relationship to Nanostructural Characteristics across a Human Osteon. IFMBE Proceedings, 2010, , 190-192.	0.3	0
144	Impact of a multi-frequency sequence of measurements on first arriving signal velocity on a bone		2

plate model. , 2009, , .

PAS	CAL	Lau	GI	ER
	0/12	2,104		

#	Article	IF	CITATIONS
145	Influence of the filling fluid on frequency-dependent velocity and attenuation in cancellous bones between 0.35 and 2.5 MHz. Journal of the Acoustical Society of America, 2009, 126, 3301-3310.	1.1	37
146	Characterizing Biot constants from ultrasound through trabecular bone. , 2009, , .		1
147	Three-dimensional high-frequency characterization of excised human lymph nodes. , 2009, , .		4
148	Analysis of the most energetic late arrival in axially transmitted signals in cortical bone. IEEE Transactions on Ultrasonics, Ferroelectrics, and Frequency Control, 2009, 56, 2463-2470.	3.0	26
149	Texture analysis using Nakagami-MRF model: Preliminary results on ultrasound images of primary choroidal melanomas. , 2009, , .		2
150	Assessment of Microelastic Properties of Bone Using Scanning Acoustic Microscopy: A Face-to-Face Comparison with Nanoindentation. Japanese Journal of Applied Physics, 2009, 48, 07GK01.	1.5	36
151	High-Frequency Quantitative Ultrasound Imaging of Cancerous Lymph Nodes. Japanese Journal of Applied Physics, 2009, 48, 07GK08.	1.5	12
152	Comparative ultrasound evaluation of human trabecular bone graft properties after treatment with different sterilization procedures. Journal of Biomedical Materials Research - Part B Applied Biomaterials, 2009, 90B, 430-437.	3.4	17
153	In vivo Performance Evaluation of Bi-Directional Ultrasonic Axial Transmission for Cortical Bone Assessment. Ultrasound in Medicine and Biology, 2009, 35, 912-919.	1.5	82
154	Assessment of cortical bone elasticity and strength: Mechanical testing and ultrasound provide complementary data. Medical Engineering and Physics, 2009, 31, 1140-1147.	1.7	50
155	Relationship between ultrasonic parameters and apparent trabecular bone elastic modulus: A numerical approach. Journal of Biomechanics, 2009, 42, 2033-2039.	2.1	44
156	Periodicity estimation under variations of scatterer spacings, thickness and pulse frequency: A 2D simulation study. , 2009, , .		3
157	Propagation of two longitudinal waves in human cancellous bone: An <i>in vitro</i> study. Journal of the Acoustical Society of America, 2009, 125, 3460-3466.	1.1	79
158	Extracting fast and slow wave velocities and attenuations from experimental measurements of cancellous bone using Bayesian probability theory. , 2009, , .		1
159	DECOMPOSITION OF INTERFERING ULTRASONIC WAVES IN BONE AND BONE-MIMICKING MATERIALS. AIP Conference Proceedings, 2009, , .	0.4	3
160	Nonlinear ultrasound can detect accumulated damage in human bone. Journal of Biomechanics, 2008, 41, 1062-1068.	2.1	38
161	Prediction of bone mechanical properties using QUS and pQCT: Study of the human distal radius. Medical Engineering and Physics, 2008, 30, 761-767.	1.7	41
162	In Vivo Measurements of Ultrasound Transmission Through the Human Proximal Femur. Ultrasound in Medicine and Biology, 2008, 34, 1186-1190.	1.5	29

#	Article	IF	CITATIONS
163	Fast wave ultrasonic propagation in trabecular bone: Numerical study of the influence of porosity and structural anisotropy. Journal of the Acoustical Society of America, 2008, 123, 1694-1705.	1.1	88
164	Application of Biot's theory to ultrasonic characterization of human cancellous bones: Determination of structural, material, and mechanical properties. Journal of the Acoustical Society of America, 2008, 123, 2415-2423.	1.1	52
165	Singular value decomposition-based wave extraction in axial transmission: application to cortical bone ultrasonic characterization [correspondence]. IEEE Transactions on Ultrasonics, Ferroelectrics, and Frequency Control, 2008, 55, 1328-1332.	3.0	27
166	Relationships of trabecular bone structure with quantitative ultrasound parameters: In vitro study on human proximal femur using transmission and backscatter measurements. Bone, 2008, 42, 1193-1202.	2.9	84
167	Spatial distribution of anisotropic acoustic impedance assessed by time-resolved 50-MHz scanning acoustic microscopy and its relation to porosity in human cortical bone. Bone, 2008, 43, 187-194.	2.9	32
168	Instrumentation for in vivo ultrasonic characterization of bone strength. IEEE Transactions on Ultrasonics, Ferroelectrics, and Frequency Control, 2008, 55, 1179-1196.	3.0	136
169	Sensitivity of QUS parameters to controlled variations of bone strength assessed with a cellular model. IEEE Transactions on Ultrasonics, Ferroelectrics, and Frequency Control, 2008, 55, 1488-1496.	3.0	24
170	Modeling the impact of soft tissue on axial transmission measurements of ultrasonic guided waves in human radius. Journal of the Acoustical Society of America, 2008, 124, 2364-2373.	1.1	50
171	Velocity dispersion in trabecular bone: Influence of multiple scattering and of absorption. Journal of the Acoustical Society of America, 2008, 124, 4047-4058.	1.1	66
172	Model-based estimation of quantitative ultrasound variables at the proximal femur. IEEE Transactions on Ultrasonics, Ferroelectrics, and Frequency Control, 2008, 55, 1304-1315.	3.0	19
173	Three-dimensional segmentation of high-frequency ultrasound echo signals from dissected lymph nodes. , 2008, , .		15
174	Derivation of the mesoscopic elasticity tensor of cortical bone from quantitative impedance images at the micron scale. Computer Methods in Biomechanics and Biomedical Engineering, 2008, 11, 147-157.	1.6	22
175	How does ultrasound bidirectional axial transmission reflect geometry of long bones?. , 2008, , .		1
176	Upper limb muscle forces: A comparative study. Computer Methods in Biomechanics and Biomedical Engineering, 2008, 11, 147-148.	1.6	6
177	Ultrasonic Propagation Through Trabecular Bone Modeled as a Random Medium. Japanese Journal of Applied Physics, 2008, 47, 4220.	1.5	9
178	Introduction to the special issue on diagnostic and therapeutic applications of ultrasound in bone - Part I. IEEE Transactions on Ultrasonics, Ferroelectrics, and Frequency Control, 2008, 55, 1177-1178.	3.0	5
179	A device for in vivo measurements of quantitative ultrasound variables at the human proximal femur. IEEE Transactions on Ultrasonics, Ferroelectrics, and Frequency Control, 2008, 55, 1197-1204.	3.0	39
180	Comparison of the Faran Cylinder Model and the Weak Scattering Model for predicting the frequency dependence of backscatter from human cancellous femur in vitro. Journal of the Acoustical Society of America, 2008, 124, 1408-1410.	1.1	9

#	Article	IF	CITATIONS
181	Additive Effect of RGD Coating to Functionalized Titanium Surfaces on Human Osteoprogenitor Cell Adhesion and Spreading. Tissue Engineering - Part A, 2008, 14, 1445-1455.	3.1	38
182	Introduction to the special issue on diagnostic and therapeutic applications of ultrasound in bone-part II. IEEE Transactions on Ultrasonics, Ferroelectrics, and Frequency Control, 2008, 55, 1415-1416.	3.0	3
183	P5A-5 Dependence of Both Slow and Fast Wave Mode Properties on Bone Volume Fraction and Structural Anisotropy in Human Trabecular Bone: A 3D Simulation Study. Proceedings IEEE Ultrasonics Symposium, 2007, , .	0.0	0
184	Effect of porosity on effective diagonal stiffness coefficients (cii) and elastic anisotropy of cortical bone at 1MHz: A finite-difference time domain study. Journal of the Acoustical Society of America, 2007, 122, 1810-1817.	1.1	43
185	P1A-7 Automatic Segmentation of the Anterior Chamber in In Vivo High-Frequency Ultrasound Images of the Eye. Proceedings IEEE Ultrasonics Symposium, 2007, , .	0.0	2
186	P6C-3 Quantitative Ultrasonography Of Choroidal Melanoma Following Proton-Beam Radiotherapy. , 2007, , .		0
187	P5A-8 Spatial Distribution of Acoustic Impedance and Microstructure Assessed by Scanning Acoustic Microscopy in Human Radial Cortical Bone. Proceedings IEEE Ultrasonics Symposium, 2007, , .	0.0	0
188	Application of nonlinear dynamics to monitoring progressive fatigue damage in human cortical bone. Applied Physics Letters, 2007, 91, .	3.3	28
189	12C-1 High Resolution Acoustic Microscopy: A New Method to Investigate Remodeling Process of Trabecular Bone. Proceedings IEEE Ultrasonics Symposium, 2007, , .	0.0	1
190	Ultrasonically determined thickness of long cortical bones: Three-dimensional simulations of in vitro experiments. Journal of the Acoustical Society of America, 2007, 122, 2439-2445.	1.1	44
191	Ultrasonically determined thickness of long cortical bones: Two-dimensional simulations ofin vitroexperiments. Journal of the Acoustical Society of America, 2007, 122, 1818-1826.	1.1	45
192	A method for the estimation of femoral bone mineral density from variables of ultrasound transmission through the human femur. Bone, 2007, 40, 37-44.	2.9	56
193	Variations of microstructure, mineral density and tissue elasticity in B6/C3H mice. Bone, 2007, 41, 1017-1024.	2.9	36
194	Attenuation in trabecular bone: A comparison between numerical simulation and experimental results in human femur. Journal of the Acoustical Society of America, 2007, 122, 2469-2475.	1.1	59
195	Quantitative Echography in the Follow-Up of Patients Treated with Proton-Beam Irradiation for Primary Choroidal Melanomas. Ultrasound in Medicine and Biology, 2007, 33, 1046-1056.	1.5	6
196	Computer simulations of ultrasonic propagation in trabecular bone. Computers in Biology and Medicine, 2007, 37, 1827-1828.	7.0	1
197	Apparent Young's modulus of human radius using inverse finite-element method. Journal of Biomechanics, 2007, 40, 2022-2028.	2.1	59
198	Wavelet-Based Signal Processing of In Vitro Ultrasonic Measurements at the Proximal Femur. Ultrasound in Medicine and Biology, 2007, 33, 970-980.	1.5	17

#	Article	IF	CITATIONS
199	Variation of Ultrasonic Parameters With Microstructure and Material Properties of Trabecular Bone: A 3D Model Simulation. Journal of Bone and Mineral Research, 2007, 22, 665-674.	2.8	112
200	Effects of gamma irradiation on mechanical properties of defatted trabecular bone allografts assessed by speed-of-sound measurement. Cell and Tissue Banking, 2007, 8, 205-210.	1.1	16
201	Effects of frequency-dependent attenuation and velocity dispersion on in vitro ultrasound velocity measurements in intact human femur specimens. IEEE Transactions on Ultrasonics, Ferroelectrics, and Frequency Control, 2006, 53, 39-51.	3.0	54
202	Experimental evaluation of bone quality measuring speed of sound in cadaver mandibles. Oral Surgery Oral Medicine Oral Pathology Oral Radiology and Endodontics, 2006, 102, 782-791.	1.4	21
203	Numerical simulation of wave propagation in cancellous bone. Ultrasonics, 2006, 44, e239-e243.	3.9	27
204	Bone micro-damage assessment using non-linear resonant ultrasound spectroscopy (NRUS) techniques: A feasibility study. Ultrasonics, 2006, 44, e245-e249.	3.9	16
205	Influence of the precision of spectral backscatter measurements on the estimation of scatterers size in cancellous bone. Ultrasonics, 2006, 44, e57-e60.	3.9	14
206	High-frequency ultrasound detection and follow-up of Wilms' tumor in the mouse. Ultrasound in Medicine and Biology, 2006, 32, 183-190.	1.5	21
207	Characterization of in vitro healthy and pathological human liver tissue periodicity using backscattered ultrasound signals. Ultrasound in Medicine and Biology, 2006, 32, 649-657.	1.5	41
208	Statut osseux au cours de l'hyperparathyroÃ⁻die primitive mesurée par densité minérale osseuse régionale par densitométrie corps entier et ultrasonographie quantitative au calcanéum. Revue Du Rhumatisme (Edition Francaise), 2006, 73, 83-92.	0.0	1
209	Assessment of bone structure and acoustic impedance in C3H and BL6 mice using high resolution scanning acoustic microscopy. Ultrasonics, 2006, 44, e1307-e1311.	3.9	12
210	Numerical simulation of the dependence of quantitative ultrasonic parameters on trabecular bone microarchitecture and elastic constants. Ultrasonics, 2006, 44, e289-e294.	3.9	24
211	Bone status in primary hyperparathyroidism assessed by regional bone mineral density from the whole body scan and QUS imaging at calcaneus. Joint Bone Spine, 2006, 73, 86-94.	1.6	9
212	Quantitative ultrasound ofÂbone: looking ahead. Joint Bone Spine, 2006, 73, 125-128.	1.6	52
213	Simulation of Ultrasound Propagation Through Three-Dimensional Trabecular Bone Structures: Comparison with Experimental Data. Japanese Journal of Applied Physics, 2006, 45, 6496-6500.	1.5	24
214	Site-matched assessment of structural and tissue properties of cortical bone using scanning acoustic microscopy and synchrotron radiation 1¼CT. Physics in Medicine and Biology, 2006, 51, 733-746.	3.0	75
215	Modelling Nonlinear Ultrasound Propagation in Bone. AIP Conference Proceedings, 2006, , .	0.4	2
216	Ultrasonic Backscatter and Attenuation (11–27 MHz) Variation with Collagen Fiber Distribution in Ex Vivo Human Dermis. Ultrasonic Imaging, 2006, 28, 23-40.	2.6	25

#	Article	IF	CITATIONS
217	Estimation of Trabecular Thickness Using Ultrasonic Backcatter. Ultrasonic Imaging, 2006, 28, 3-22.	2.6	36
218	Derivation of elastic stiffness from site-matched mineral density and acoustic impedance maps. Physics in Medicine and Biology, 2006, 51, 747-758.	3.0	95
219	In vitroultrasonic characterization of human cancellous femoral bone using transmission and backscatter measurements: Relationships to bone mineral density. Journal of the Acoustical Society of America, 2006, 119, 654-663.	1.1	75
220	2A-6 Optimization Algorithm for Improved Quantitative Ultrasound Signal Processing at the Proximal Femur. , 2006, , .		2
221	Computation of cortical bone macroscopic properties from microscopic elastic data. , 2006, , 591-591.		0
222	Monitoring cell adhesion processes on bioactive polymers with the quartz crystal resonator technique. Biomaterials, 2005, 26, 4197-4205.	11.4	35
223	In vitro chronic hepatic disease characterization with a multiparametric ultrasonic approach. Ultrasonics, 2005, 43, 305-313.	3.9	53
224	Comparison of three ultrasonic axial transmission methods for bone assessment. Ultrasound in Medicine and Biology, 2005, 31, 633-642.	1.5	105
225	Bone microstructure and elastic tissue properties are reflected in QUS axial transmission measurements. Ultrasound in Medicine and Biology, 2005, 31, 1225-1235.	1.5	121
226	Optimal Prediction of Bone Mineral Density with Ultrasonic Measurements in Excised Human Femur. Calcified Tissue International, 2005, 77, 186-192.	3.1	40
227	Appropriateness of internal digital phantoms for monitoring the stability of the UBIS 5000 quantitative ultrasound device in clinical trials. Osteoporosis International, 2005, 16, 435-445.	3.1	8
228	In vitro speed of sound measurement at intact human femur specimens. Ultrasound in Medicine and Biology, 2005, 31, 987-996.	1.5	48
229	Recent developments in trabecular bone characterization using ultrasound. Current Osteoporosis Reports, 2005, 3, 64-69.	3.6	22
230	Nonlinear resonant ultrasound spectroscopy (NRUS) applied to damage assessment in bone. Journal of the Acoustical Society of America, 2005, 118, 3946-3952.	1.1	117
231	Progress towardsin vitroquantitative imaging of human femur using compound quantitative ultrasonic tomography. Physics in Medicine and Biology, 2005, 50, 2633-2649.	3.0	28
232	Dynamic coherent backscattering in a heterogeneous absorbing medium: Application to human trabecular bone characterization. Applied Physics Letters, 2005, 87, 114101.	3.3	33
233	Three-dimensional simulation of ultrasound propagation through trabecular bone structures measured by synchrotron microtomography. Physics in Medicine and Biology, 2005, 50, 5545-5556.	3.0	153
234	High-resolution ultrasonography of subretinal structure and assessment of retina degeneration in rat. Experimental Eye Research, 2005, 81, 592-601.	2.6	13

#	Article	IF	CITATIONS
235	Segmentation of Quantitative Ultrasonographic Images of the Calcaneus Using Elastic Deformation of the Flexible Fourier Contour. Journal of Ultrasound in Medicine, 2004, 23, 693-699.	1.7	3
236	High resolution ultrasound elastomicroscopy imaging of soft tissues: system development and feasibility. Physics in Medicine and Biology, 2004, 49, 3925-3938.	3.0	35
237	High-Resolution Ultrasonography for Analysis of Age- and Disease-Related Cartilage Changes. , 2004, 101, 249-266.		3
238	Bidirectional axial transmission can improve accuracy and precision of ultrasonic velocity measurement in cortical bone: a validation on test materials. IEEE Transactions on Ultrasonics, Ferroelectrics, and Frequency Control, 2004, 51, 71-79.	3.0	122
239	Three-dimensional simulations of ultrasonic axial transmission velocity measurement on cortical bone models. Journal of the Acoustical Society of America, 2004, 115, 2314-2324.	1.1	248
240	An In Vitro Study of the Ultrasonic Axial Transmission Technique at the Radius: 1-MHz Velocity Measurements Are Sensitive to Both Mineralization and Intracortical Porosity. Journal of Bone and Mineral Research, 2004, 19, 1548-1556.	2.8	109
241	In Vitro Ultrasound Measurement at the Human Femur. Calcified Tissue International, 2004, 75, 421-430.	3.1	27
242	2D arrays device for calcaneus bone transmission: an alternative technological solution using crossed beam forming. Ultrasonics, 2004, 42, 745-752.	3.9	12
243	Cell Attachment and Spreading Processes Monitored by the Thickness Shear-Mode Quartz Sensor. IEEE Sensors Journal, 2004, 4, 535-542.	4.7	13
244	Singular spectrum analysis applied to backscattered ultrasound signals from in vitro human cancellous bone specimens. IEEE Transactions on Ultrasonics, Ferroelectrics, and Frequency Control, 2004, 51, 302-312.	3.0	53
245	An overview of bone sonometry. International Congress Series, 2004, 1274, 23-32.	0.2	33
246	Singular spectrum analysis applied to backscattered ultrasound signals from in vitro human cancellous bone specimens. IEEE Transactions on Ultrasonics, Ferroelectrics, and Frequency Control, 2004, 51, 302-12.	3.0	10
247	Parametric analysis of carotid plaque using a clinical ultrasound imaging system. Ultrasound in Medicine and Biology, 2003, 29, 1521-1530.	1.5	23
248	Effects of antiinflammatory drugs on arthritic cartilage: A high-frequency quantitative ultrasound study in rats. Arthritis and Rheumatism, 2003, 48, 1594-1601.	6.7	28
249	Prediction of frequency-dependent ultrasonic backscatter in cancellous bone using statistical weak scattering model. Ultrasound in Medicine and Biology, 2003, 29, 455-464.	1.5	67
250	Optimization of attenuation estimation in reflection for in vivo human dermis characterization at 20 MHz. IEEE Transactions on Ultrasonics, Ferroelectrics, and Frequency Control, 2003, 50, 408-418.	3.0	15
251	Milestones on the road to higher resolution, quantitative, and functional ultrasonic imaging. Proceedings of the IEEE, 2003, 91, 1543-1561.	21.3	21
252	Prediction of backscatter coefficient in trabecular bones using a numerical model of three-dimensional microstructure. Journal of the Acoustical Society of America, 2003, 113, 1122-1129.	1.1	59

#	Article	IF	CITATIONS
253	Effect of bone cortical thickness on velocity measurements using ultrasonic axial transmission: A 2D simulation study. Journal of the Acoustical Society of America, 2002, 112, 297-307.	1.1	173
254	Ultrasonic characterization of human cancellous bone using transmission and backscatter measurements: relationships to density and microstructure. Bone, 2002, 30, 229-237.	2.9	179
255	20-MHZ US Backscatter Measurements and Reproducibility: Normal Human Dermis in Vivo. , 2002, , 303-308.		0
256	Effect of articular cartilage proteoglycan depletion on high frequency ultrasound backscatter. Osteoarthritis and Cartilage, 2002, 10, 535-541.	1.3	60
257	In vivo performance of a matrix-based quantitative ultrasound imaging device dedicated to calcaneus investigation. Ultrasound in Medicine and Biology, 2002, 28, 1285-1293.	1.5	25
258	Singular Spectrum Analysis Applied to 20MHz Backscattered Ultrasound Signals from Periodic and Quasi-Periodic Phantoms. Acoustical Imaging, 2002, , 239-246.	0.2	10
259	2D Simulation of the Axial Transmission Technique on a Cortical Bone Plate. Acoustical Imaging, 2002, , 69-76.	0.2	2
260	Application of Short-Time Fourier Multi-Narrowband Analysis to In Vivo Human Skin Between 12 and 25 MHz. Acoustical Imaging, 2002, , 167-173.	0.2	0
261	Quantitative Ultrasound for Bone Properties. Acoustical Imaging, 2002, , 45-52.	0.2	0
262	Reproducibility of skin characterization with backscattered spectra (12–25 MHz) in healthy subjects. Ultrasound in Medicine and Biology, 2001, 27, 603-610.	1.5	35
263	Ultrasonic Backscatter and Transmission Parameters at the Os Calcis in Postmenopausal Osteoporosis. Journal of Bone and Mineral Research, 2001, 16, 1353-1362.	2.8	91
264	Assessment of rat articular cartilage maturation using 50-MHz quantitative ultrasonography. Osteoarthritis and Cartilage, 2001, 9, 178-186.	1.3	60
265	Computerized ultrasound B-scan characterization of breast nodules. Ultrasound in Medicine and Biology, 2000, 26, 1421-1428.	1.5	64
266	Quantitative Ultrasound Imaging of the Calcaneus: Precision and Variations During a 120-Day Bed Rest. Calcified Tissue International, 2000, 66, 16-21.	3.1	17
267	Phase and group velocities of fast and slow compressional waves in trabecular bone. Journal of the Acoustical Society of America, 2000, 108, 1949-1952.	1.1	56
268	Analysis of the axial transmission technique for the assessment of skeletal status. Journal of the Acoustical Society of America, 2000, 108, 3058-3065.	1.1	80
269	Evaluation of Error Bounds on Calcaneal Speed of Sound Caused by Surrounding Soft Tissue. Journal of Clinical Densitometry, 2000, 3, 121-131.	1.2	43
270	In vitro measurement of the frequency-dependent attenuation in cancellous bone between 0.2 and 2 MHz. Journal of the Acoustical Society of America, 2000, 108, 1281.	1.1	112

Pascal Laugier

#	Article	IF	CITATIONS
271	Ultrasound Measurement on the Calcaneus: Influence of Immersion Time and Rotation of the Foot. Osteoporosis International, 1999, 9, 318-326.	3.1	48
272	In Vivo Results with a New Device for Ultrasonic Monitoring of Pig Skin Cryosurgery: The Echographic Cryoprobe. Journal of Investigative Dermatology, 1998, 111, 314-319.	0.7	10
273	Evaluation of Acoustical Parameter Sensitivity to Age-Related and Osteoarthritic Changes in Articular Cartilage Using 50-MHz Ultrasound. Ultrasound in Medicine and Biology, 1998, 24, 341-354.	1.5	122
274	Automatic detection of the boundary of the calcaneus from ultrasound parametric images using an active contour model; clinical assessment. IEEE Transactions on Medical Imaging, 1998, 17, 45-52.	8.9	48
275	Velocity dispersion of acoustic waves in cancellous bone. IEEE Transactions on Ultrasonics, Ferroelectrics, and Frequency Control, 1998, 45, 581-592.	3.0	154
276	In vitro assessment of the relationship between acoustic properties and bone mass density of the calcaneus by comparison of ultrasound parametric imaging and quantitative computed tomography. Bone, 1997, 20, 157-165.	2.9	170
277	Assessment of Articular Cartilage and Subchondral Bone: Subtle and Progressive Changes in Experimental Osteoarthritis Using 50 MHz Echography In Vitro. Journal of Bone and Mineral Research, 1997, 12, 1378-1386.	2.8	82
278	Assessment of the relationship between broadband ultrasound attenuation and bone mineral density at the calcaneus using BUA imaging and DXA. Osteoporosis International, 1997, 7, 316-322.	3.1	97
279	Quantitative ultrasound imaging at the calcaneus using an automatic region of interest. Osteoporosis International, 1997, 7, 363-369.	3.1	61
280	Absolute backscatter coefficient over a wide range of frequencies in a tissue-mimicking phantom containing two populations of scatterers. IEEE Transactions on Ultrasonics, Ferroelectrics, and Frequency Control, 1996, 43, 970-978.	3.0	64
281	Ultrasound Parametric Imaging of the Calcaneus: In Vivo Results with a New Device. Calcified Tissue International, 1996, 58, 326-331.	3.1	12
282	Broadband ultrasound attenuation imaging: A new imaging method in osteoporosis. Journal of Bone and Mineral Research, 1996, 11, 1112-1118.	2.8	81
283	In Vitro and in Vivo Assessment of Ultrasound Parametric Images of Bone. Acoustical Imaging, 1996, , 311-318.	0.2	3
284	Application of autoregressive spectral analysis for ultrasound attenuation estimation: interest in highly attenuating medium. IEEE Transactions on Ultrasonics, Ferroelectrics, and Frequency Control, 1995, 42, 99-110.	3.0	60
285	Broadband ultrasonic attenuation imaging: A new imaging technique of the os calcis. Calcified Tissue International, 1994, 54, 83-86.	3.1	71
286	Ultrasound Attenuation Imaging in the Os Calcis: An Improved Method. Ultrasonic Imaging, 1994, 16, 65-76.	2.6	31
287	Assessment of Echography as a Monitoring Technique for Cryosurgery. Ultrasonic Imaging, 1993, 15, 14-24.	2.6	5
288	INTÉRÊT ET MÉTHODOLOGIE DE L'ÉCHOGRAPHIE QUANTITATIVE. European Physical Journal Special Top	Dics, 0:2	1

ropean Physical Journa Ųι ai Speci 288 1992, 02, C1-27-C1-40.

#	Article	IF	CITATIONS
289	Partially coherent transducers: The random phase transducer approach. Ultrasonic Imaging, 1990, 12, 205-228.	2.6	5
290	Global breast attenuation: Control group and benign breast diseases. Ultrasonic Imaging, 1990, 12, 47-57.	2.6	11
291	The random phase transducer: a new technique for incoherent processing-experimental results. IEEE Transactions on Ultrasonics, Ferroelectrics, and Frequency Control, 1990, 37, 70-78.	3.0	7
292	Attenuation estimation with random phase transducers. Ultrasonic Imaging, 1988, 10, 56.	2.6	2
293	Frequency-dependent attenuation in human breast correlated to physiological parameters. Ultrasonic Imaging, 1988, 10, 56-57.	2.6	1
294	High resolution ultrasonic attenuation estimation with a random phase screen. , 1988, , .		0
295	Quantitative echography: attenuation estimation and clinical applications. , 1988, , .		0
296	Optimal precision in ultrasound attenuation estimation and application to the detection of Duchenne Muscular Dystrophy carriers. Ultrasonic Imaging, 1987, 9, 1-17.	2.6	17
297	Correlation between ultrasound attenuation in muscle and pathological fatty infiltration. Ultrasonic Imaging, 1987, 9, 66.	2.6	6
298	Diffraction correction for focused transducers in attenuation measurements ?. Ultrasonic Imaging, 1987, 9, 248-259.	2.6	15
299	In vivo variance of the attenuation in muscle with respect to theory, simulation and pathological studies (DMD). Ultrasonic Imaging, 1986, 8, 51-52.	2.6	3
300	Two solutions for the diffraction effect on in vivo attenuation measurements: In vivo filter or adaptive experimental conditions. Ultrasonic Imaging, 1986, 8, 52.	2.6	0
301	Specular reflector noise: Effect and correction for in vivo attenuation estimation. Ultrasonic Imaging, 1985, 7, 277-292.	2.6	19
302	Influence of specular reflectors on attenuation measurements in muscles. Ultrasonic Imaging, 1985, 7, 84-85.	2.6	2
303	80 MHz three-dimensional ultrasound imaging of corneal lesions induced by cataract surgery. , 0, , .		2
304	Quantitative echography: a potential control technique for cryosurgery. , 0, , .		0
305	Experimental results of ultrasonic monitoring of cryotherapy on in vitro skin samples of domestic pig. , 0, , .		1
306	Relationship between skin-collagen micro-architecture and ultrasonic backscatter parameters at 20 MHz. , 0, , .		3

#	Article	IF	CITATIONS
307	Adhesion of human osteoprogenitor cells on peptide immobilization onto titanium monitored a quartz crystal resonator technique. , 0, , .		1
308	Application of Non-Linear Elastic Wave Spectroscopy (NEWS) to In Vitro Damage Assessment in Cortical Bone. , 0, , 253-273.		0